The Effect of Initial Water Saturation on Enhanced Water Imbibition by Surfactant for Fractured Tight Porous Media

Mingyuan Wang, Francisco J. Argüelles-Vivas, Gayan A. Abeykoon, and **Ryosuke Okuno,**
University of Texas at Austin

Summary

The main objective of this research was to investigate the effect of initial water saturation on the oil recovery from tight matrices through surfactant-enhanced water imbibition. Two flooding/soaking experiments using fractured tight cores with/without initial water were performed. The experimental results were analyzed by the material balance for the components oil, brine, and surfactant. The analysis resulted in a quantitative evaluation of the imbibed fraction of the injected components (brine and surfactant).

Results show that the surfactant enhanced the brine imbibition into the matrix through wettability alteration. The initial efficiency of the surfactant imbibition increased when brine was initially present in the matrix. The imbibition of brine was more efficient with no initial water in the matrix. A possible reason is that the presence of initial water in the matrix was able to increase the initial efficiency of the surfactant imbibition; however, the increased amount of surfactant in the matrix lowered the interfacial tension (IFT) between the aqueous and oleic phases; therefore, the efficiency of brine imbibition was reduced. Another possible reason is that capillary force was lower in the presence of initial water in the matrix, resulting in weaker imbibition of brine.

Although the two cases showed different characteristics of the mass transfer through the fracture/matrix interface, they resulted in similar values of final water saturation in the matrix. Hence, the surfactant injection was more efficient for a given amount of oil recovery when there was no initial water in the matrix.

Introduction

Producing oil from tight formations at economical rates became possible because of hydraulic fracturing and horizontal drilling. However, tight reservoirs show a rapid production-rate decline and low recovery factors (less than 10%) because of the adverse petrophysical properties, such as ultralow permeability, high total organic content, and heterogeneous mineralogy (Alharthy et al. 2015; Barba 2015). Wettability measurements through contact angles indicate that tight formations are either intermediate- to oil-wet (Alvarez and Schechter 2016).

To improve oil recovery in shales, surfactant solutions have been proposed to facilitate the spontaneous imbibition of water (Morsy et al. 2013; Alvarez and Schechter 2017; Alvarez et al. 2018a, 2018b). The oil-recovery mechanisms by these additives include wettability alteration and IFT reduction between the aqueous and oleic phases (Kathel and Mohanty 2013; Alvarez et al. 2014; Alvarez and Schechter 2017; Alvarez et al. 2018a, 2018b; Zeng et al. 2018; Liu et al. 2019). For instance, Alvarez et al. (2014) showed that anionic and nonionic surfactants were able to alter the wettability of carbonate and siliceous shales from oil- to water-wet state, but anionic surfactant showed better performance as a wettability modifier. Liu et al. (2019) found that anionic surfactants modified the wettability of siliceous shales, but nonionic surfactants did not work for that purpose. Yarveicy et al. (2018) showed that the surfactant used could reduce the trapping of the aqueous phase and improved oil recovery from Montney tight cores. Yarveicy and Haghtalab (2018) and Yarveicy and Javaheri (2019) showed improved oil recovery by surfactant flooding using micromodels. Alvarez et al. (2018a) and Alvarez and Schechter (2017) emphasized that although IFT reduction is important, it should not reach ultralow values (10^{-3} mN/m) during injection of surfactant solution into shales.

Besides petrophysical properties, the production of water also represents a problem for oil recovery and field operations in tight formations. It has been reported that the water cut is 90% in part of the Permian Basin (Rassenfoss 2018) and approximately 30% for the Eagle Ford (Pettit et al. 2016). Because surfactants are injected as aqueous solutions, the effect of surfactant injection on oil recovery from a tight formation can be affected by the phase distribution in the tight matrix. It is still unknown how the initial water saturation would influence the performance of surfactant in oil recovery from tight porous media.

In the case of conventional reservoirs, it is well-documented that initial water saturation (S_{wi}) affects oil recovery and spontaneous water imbibition (Viksund et al. 1998; Cil et al. 1998; Akin et al. 2000; Zhou et al. 2000; Tong et al. 2001; Li and Li 2014; Cheng et al. 2017; Abedi et al. 2020). With Berea Sandstone, Viksund et al. (1998) found that the imbibition rate decreased as S_{wi} increased between 0 and 6%, and then it increased from 15 to 34% of S_{wi}; the oil recovery by water imbibition was slightly influenced by S_{wi} ranging from 0 to 30%. For Rørdal chalks, Viksund et al. (1998) observed that the imbibition rate increased as S_{wi} increased up to 34%, and then it decreased slightly for higher water saturations; the oil recovery reduced from 67 to 30% as the S_{wi} augmented from 7.5 to 51%.

With Berea sandstones, Cil et al. (1998) found that the oil recovery by countercurrent spontaneous imbibition was not significantly affected by S_{wi} in the range between 0 and 20%. However, the oil recovery increased for S_{wi} greater than 20%. Zhou et al. (2000) analyzed the interaction among rock wettability, S_{wi}, aging time, and oil recovery on Berea sandstones during spontaneous water imbibition and waterflooding. They observed that as the S_{wi} decreased (as a consequence of wettability change and aging time), the imbibition rate and final oil recovery also decreased. By performing imbibition experiments in diatomite cores, Akin et al. (2000) showed that oil recovery diminished as S_{wi} augmented (up to 60%). They also found that residual oil saturation was not significantly affected by S_{wi} [for recovery measured in pore volume (PV)].

Tong et al. (2001) did not observe a systematic effect of S_{wi} on oil recovery in Berea sandstones. However, oil recovery became sensitive to S_{wi} when the experiments were scaled up to reservoir conditions: It increased as S_{wi} increased in the range of 11 to 28%. Li and

This paper (SPE 200431) was accepted for presentation at the SPE Improved Oil Recovery Conference, Virtual, 31 August–4 September 2020, and revised for publication. Original manuscript received for review 26 August 2020. Revised manuscript received for review 7 October 2020. Paper peer approved 19 October 2020.

Li (2014) investigated the effects of S_{wi} on oil production by water imbibition through reservoir simulations. Unlike the results in core experiments, they found no influence of S_{wi} on oil production and oil recovery. This difference was attributed to the type of displacement: It was spontaneous imbibition at core scale, whereas it was forced imbibition at the reservoir scale. Overall, the results from these investigations show that the effects of S_{wi} on water imbibition are not well-understood so far.

Several studies also investigated the effect of initial water saturation on surfactant-enhanced water imbibition from the chalk cores (Standnes and Austad 2000; Babadagli 2005). Standnes and Austad (2000) performed spontaneous-imbibition experiments using a cationic surfactant. They observed faster spontaneous imbibition of water with the presence of initial water in the core. However, they also mentioned that their result was affected by the method of core preparation. For the core with initial water in the matrix, the brine was injected into the core before the oil. Because the core surface was first in contact with brine, the oil saturation and the amount of surface-active materials could be small near the rock surface. As a result, the core was more water-wet for the case with initial water in the matrix. Babadagli (2005) performed spontaneous-imbibition experiments with an anionic surfactant and a nonionic surfactant. He observed that oil recovery was faster with initial water in the system for the anionic surfactant. For the nonionic surfactants, however, oil recovery was slower with the presence of initial water.

In the case of shales and tight formations, studies to investigate the correlation between S_{wi} and water imbibition are scarce (Ghanbari and Dehghanpour 2015; Gao and Hu 2016). Also, a limited amount of data of S_{wi} in shales has been reported. The S_{wi} is 25% for organic Barnett Shale (Bowker 2003) and 20% for Horn River Shale (Gao and Hu 2016). In Otter Park and Evie gas shales, Ghanbari and Dehghanpour (2015) observed that the water-imbibition rate decreased by the S_{wi}, but the oil-imbibition rate was not affected. They also found that hydrophobic organic material could decrease the imbibition rate of water. Gao and Hu (2016) investigated the influence of S_{wi} and imbibing fluid on the spontaneous imbibition into Barnett Shale cores. They found that the spontaneous imbibition into shales was affected by S_{wi} and mineral composition. Gao and Hu (2016) emphasized that each shale type needs a specific study because the high heterogeneities in shales make the imbibition a complicated process. No studies have been found regarding the effect of the S_{wi} on enhanced water imbibition by surfactant solution in tight matrices; this motivated the current research. The main objective of this research was to evaluate how the presence of initial water affects the oil recovery from tight matrices by the imbibition of nonionic-surfactant solution. During surfactant-enhanced brine imbibition, the surfactant is first imbibed into the matrix to change the rock wettability. Then, brine is imbibed into the matrix to displace oil from the matrix to the fracture. Therefore, the oil recovery from the matrix depends on the mass transfer of components between the matrix and the fracture. In this research, the effect of the S_{wi} was investigated by quantifying the mass transfer of components between the matrix and the fracture using material-balance analysis during flooding/soaking experiments. This is the main novelty of this research.

Two cases were compared in this research: one without initial water in the matrix and the other with initial water in the matrix. The section Methods of Experiments and Material-Balance Analysis presents the methods for this research. The section Experimental Results and Material-Balance Analysis presents the main results of the flooding/soaking experiments and the material-balance analysis, followed by the Discussion and Conclusions sections.

Methods of Experiments and Material-Balance Analysis

This section presents the methods of experiments and material-balance analysis for this study. The main experimental data were obtained through two sets of flooding/soaking experiments with 1.0-wt% surfactant solution in reservoir brine (RB) at 347 K. Properties of reservoir fluids used in this study were presented in Wang et al. (2019a, 2019b) and are not entirely duplicated here.

Surfactant Formulation. The surfactant solution used in this research is 1.0-wt% 2-ethylhexanol (EH)-4 propylene oxide (PO)-15 ethylene oxide (EO), which is a short-hydrophobe nonionic surfactant (Wang et al. 2019b). The surfactant has a purity of 99.9%.

Fig. 1 shows the contact-angle experiment performed on an oil-aged calcite surface with the 1.0-wt% surfactant solution at 347 K and atmospheric pressure (Wang et al. 2019b). The initial contact angle clearly indicated that the calcite surface was oil-wet. The average contact angle changed from 134 to 47° within 1 day. The surfactant can decrease the IFT between the aqueous and oleic phases from 11.44 to 0.21 mN/m at 347 K and atmospheric pressure (Wang et al. 2019b). Phase-behavior study showed a small amount of macroemulsion near the interface between the aqueous phase and the oleic phase (Wang et al. 2019b).

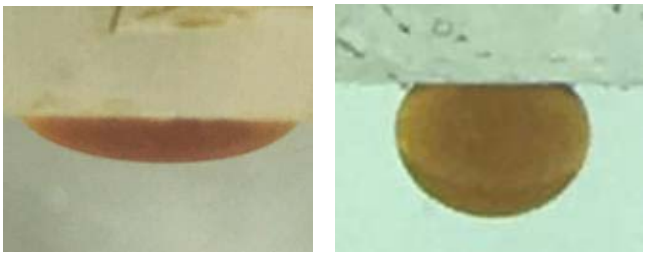

(a) Initial (b) 24 hours

Fig. 1—Contact angles at (a) the start of the experiment and (b) 24 hours after the calcite piece was immersed in 2-EH-4PO-15EO solution at 347 K and atmospheric pressure (after Wang et al. 2019b).

Experimental Procedure for Flooding/Soaking Experiments. Two horizontal flooding/soaking experiments were performed at 347 K with fractured tight carbonate cores: Case 1 with initial water in the matrix and Case 2 without initial water in the matrix. This subsection describes the preparation of the tight cores and the flooding/soaking experiments. Properties of the tight carbonate cores and the injection scheme for two flooding/soaking experiments are also summarized in this subsection.

Rocherons carbonate cores were used in this research. Because of their ultralow permeability and heterogeneity, the Rocherons cores were cut into small pieces that were 0.0254 m in diameter and approximately 0.0127 m in length before saturation with any fluids. In this research, 11 core pieces were saturated only by crude oil and five core pieces were saturated by both crude oil and RB at room temperature. To saturate the core pieces with crude oil, they were placed in an accumulator, which was evacuated for at least 24 hours.

Then, the crude oil was transferred into the accumulator, and the pressure inside the accumulator was set at 34 474 kPa for more than 40 hours. The weights of the core pieces were measured before and after saturation with crude oil to quantify the oil volume in the cores. The volume so determined was assumed to be the accessible PV of the core. Oil-saturated core pieces were then placed inside a core holder and flooded by RB under the pressure difference of 6895 kPa. **Fig. 2** shows a schematic of the brine-flooding system used. It consists of an accumulator for RB, a pump, a Hassler-type core holder, a hydraulic manual pump to maintain the overburden pressure, and cylinders. Before brine injection, the inlet tubing of the core holder was evacuated for 10 seconds to prevent injecting air into the core. The core was flooded by brine until the injected brine volume exceeded the accessible PV. After that, the core pieces were placed inside an accumulator filled with crude oil at 34 474 psi for 14 hours. The weights of the core pieces were measured after they were resaturated with the crude oil. The brine and oil volumes in the core pieces were calculated using

$$(\mathrm{PV} - V_w)\rho_o + V_w\rho_w = M_f, \quad \ldots\ldots (1)$$

$$V_o = \mathrm{PV} - V_w, \quad \ldots\ldots (2)$$

where PV is the accessible PV, V_w is the brine volume in the core piece, V_o is the oil volume in the core piece, ρ_w is the reservoir-brine density (1040 kg/m^3) at room temperature (296 K) and atmospheric pressure, ρ_o is the crude-oil density (817 kg/m^3) at room temperature (296 K) and atmospheric pressure, and M_f is the total mass of fluid in the core piece. Then, oil and brine saturations in each core piece can be calculated. In this process, the core piece was saturated with oil before brine to ensure that the rock surface was wet by oil. **Table 1** presents the properties of the core pieces, including the length of each core piece, accessible PV, and oil and brine saturations. Core Pieces 1 through 5 in Table 1 were saturated by both brine and oil. Core Pieces 6 through 16 were saturated by only oil; hence, only the first step of oil saturation was performed (without the brine flooding and the oil resaturation). We attempted to prepare more pieces that were saturated with water and oil, but multiple core pieces were broken during the water injection. This resulted in only five core pieces with nonzero initial water saturation.

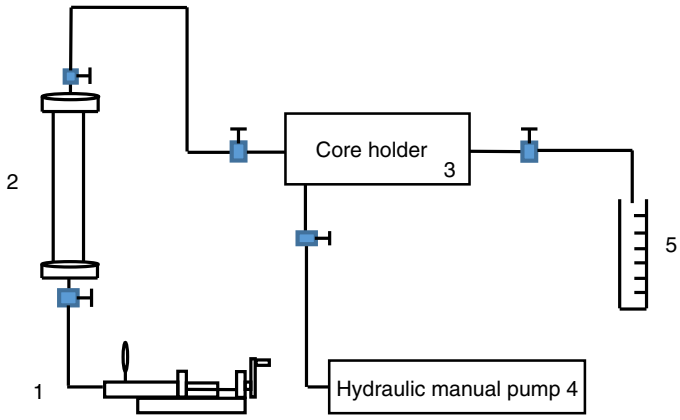

Fig. 2—Schematic of the brine-flooding system.

An artificial fracture was created along the longitudinal axis using an electric saw for each core piece. Polytetrafluoroethylene (PTFE) spacers that were 0.001 m in width were placed along two edges of the fracture to maintain a fracture aperture (Mejia 2018). Then, the core halves were carefully put together with the PTFE spacers placed in the fracture, wrapped with a PTFE tube, and placed inside a horizontally oriented core holder, with the fracture vertically oriented. No PTFE spacer was placed in the space between core pieces. **Fig. 3** shows that Core Pieces 1 through 5 were put together for Case 1 with initial water in the core, and Core Pieces 6 through 16 were put together for Case 2 without initial water in the core. When assembling the core pieces for Case 1, core pieces were put so that oil saturation changes monotonically. **Table 2** summarizes the properties of Core Pieces 1 through 5 and 6 through 16. The initial wettability of the carbonate-core pieces should be oil-wet according to the contact-angle results in the subsection Surfactant Formulation.

Fig. 4 presents a schematic of the experimental setup for the flooding/soaking experiment. It consisted of accumulators for crude oil, RB, and surfactant solution (2-EH-4PO-15EO), a pump, a Hassler-type core-holder, a hydraulic manual pump to maintain the overburden pressure, a differential pressure gauge, cylinders, and an oven. After a fractured core was placed in the core holder, the oven temperature was increased to reservoir temperature (347 K). Then, the system was evacuated for 10 seconds to remove any air trapped in the fractures. After that, the core was flooded with crude oil to measure the fracture permeability by using the flow rate of 500 cm^3/h under a certain overburden pressure. Table 2 provides the pressure drops along the cores at a certain flow rate and the overburden pressures used.

The permeabilities of the main longitudinal fracture were calculated by the method used by Mejia (2018). The equation for flow between parallel plates,

$$b = (3\pi d k_e)^{\frac{1}{3}}, \quad \ldots\ldots (3)$$

was used to estimate a fracture aperture, where b is the fracture aperture, d is the core diameter, and k_e is the effective oil permeability of the fractured core. The fracture apertures are provided in Table 2. A fracture permeability can be calculated from the fracture aperture using

$$k_f = b^2/12. \quad \ldots\ldots (4)$$

Core Piece Number	Length (m)	Accessible PV before Cutting (m^3)	Accessible PV after Cutting (m^3)	Brine Saturation	Oil Saturation
1	0.0110	6.0702×10^{-8}	5.7527×10^{-8}	0.5765	0.4235
2	0.0110	7.0493×10^{-8}	6.7718×10^{-8}	0.0636	0.9364
3	0.0100	5.4339×10^{-8}	5.1813×10^{-8}	0.0660	0.9340
4	0.0100	5.9234×10^{-8}	5.5982×10^{-8}	0.1969	0.8031
5	0.0100	5.0422×10^{-8}	4.8560×10^{-8}	0.1068	0.8932
6	0.0105	5.4094×10^{-8}	5.1438×10^{-8}	0.0000	1.0000
7	0.0115	6.1926×10^{-8}	5.8697×10^{-8}	0.0000	1.0000
8	0.0105	5.3604×10^{-8}	5.1109×10^{-8}	0.0000	1.0000
9	0.0105	5.8010×10^{-8}	5.5751×10^{-8}	0.0000	1.0000
10	0.0120	6.9759×10^{-8}	6.6633×10^{-8}	0.0000	1.0000
11	0.0100	5.2870×10^{-8}	5.0627×10^{-8}	0.0000	1.0000
12	0.0100	5.7521×10^{-8}	5.5200×10^{-8}	0.0000	1.0000
13	0.0100	6.0213×10^{-8}	5.7539×10^{-8}	0.0000	1.0000
14	0.0100	5.1157×10^{-8}	4.7916×10^{-8}	0.0000	1.0000
15	0.0100	5.4094×10^{-8}	5.2121×10^{-8}	0.0000	1.0000
16	0.0110	5.5807×10^{-8}	5.1379×10^{-8}	0.0000	1.0000

Table 1—Properties of the core pieces. Core Pieces 1 through 5 were saturated with both brine and oil. Core Pieces 6 through 16 were saturated with only oil.

(a) (b)

Fig. 3—Assembled cores for two flooding/soaking experiments. (a) Core Pieces 1 through 5 were put together for the case with initial water in the matrix (Case 1). (b) Core Pieces 6 through 16 were put together for the case without initial water in the matrix (Case 2).

	Core Pieces 1 through 5 (Case 1)	Core Pieces 6 through 16 (Case 2)
Oil volume in matrix at 347 K and atmospheric pressure (m^3)	0.2351×10^{-6}	0.6268×10^{-6}
Pressure drop along the core at 500 cm^3/h (kPa)	4.0272	6.5845
Overburden pressure (kPa)	6895	6205
Main longitudinal fracture aperture (m)	0.8788×10^{-4}	0.9742×10^{-4}
Main longitudinal fracture permeability (darcies)	652	801

Table 2—Properties of Core Pieces 1 through 5 and Core Pieces 6 through 16.

During flooding/soaking experiments, the RB was injected at 6 cm^3/h until no more oil production was observed. Then, the surfactant solution was injected at 6 cm^3/h to fill the volume from the inlet of the core holder until the outlet line of the core holder, which was followed by a 10-hour soaking period. After that, the surfactant solution was injected at 6 cm^3/h to chase the fluid in the system and to recover the produced oil during the first soaking period. The system was then shut in for a second 10-hour soaking period. RB was then injected at 6 cm^3/h to chase the fluid in the system and to recover the produced oil during the second soaking period. Finally, the system was shut in for a 12-hour soaking period, followed by RB injection to chase the fluid in the system until there was no oil production.

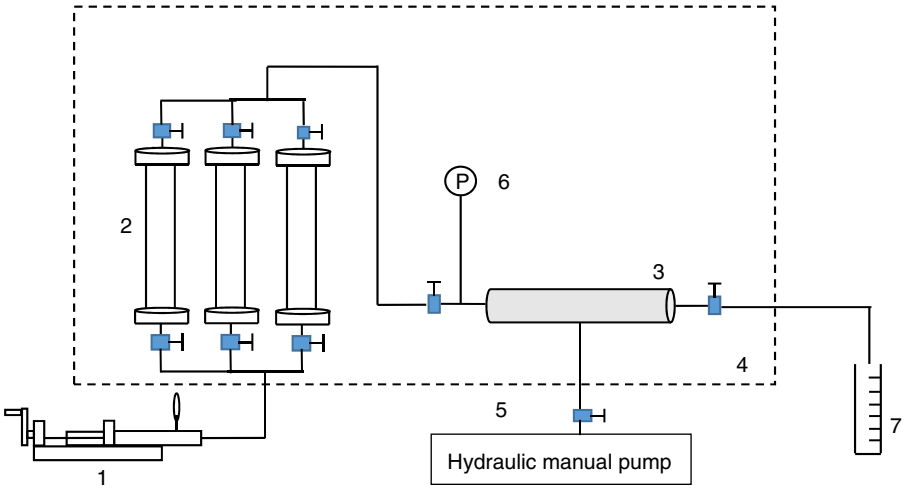

1. Pressurization pump 2. Accumulators 3. Hassler-type core holder 4. Oven
5. Hydraulic manual pump 6. Pressure gauge 7. Graduating cylinder

Fig. 4—Schematic of the experimental setup for flooding/soaking experiments.

The effluent was collected in plastic graduating cylinders at room temperature. Emulsion was observed in the graduating cylinder. A small amount of sodium chloride was added into the graduating cylinder to separate the oleic and aqueous phases. Because macroemulsions are typically larger than 1 μm, which exceeds the size of nanopores, the observed emulsion was likely generated in the fracture or the outlet tubing of the core holder, not in the matrix. The 2-EH-4PO-15EO concentration in the produced aqueous phase was measured using high-performance liquid chromatography. The concentration data were used to analyze the material balance for each flooding/soaking experiment.

Material Balance for a Fractured Core. The flooding/soaking-experiment results were analyzed by the material balance for (pseudo)components: brine, oil, and chemical. The main focus of the analysis was on the fractional amount of the injected component (brine or chemical) that was imbibed into the matrix from the fracture.

The material balance for (pseudo)component i ($i = 1$ for brine, 2 for oil, and 3 for chemical) for the dynamic imbibition **(Fig. 5)** was based on the following assumptions:

- The system volume consists of two subvolumes: the fracture volume (V_f) and the matrix volume (V_m).
- The fracture volume is connected to the injector (source) and the producer (sink).
- The system is closed except for the injector and producer.
- No chemical reaction.

For a given time interval Δt,

$$\Delta M_{fi} = M_{ti} + M_{Ii} + M_{Pi}, \quad \ldots\ldots (5)$$

$$\Delta M_{mi} = -M_{ti}, \quad \ldots\ldots (6)$$

where ΔM_{fi} and ΔM_{mi} are the accumulation of component i in V_f and V_m, respectively. M_{Ii} is the amount of component i going into V_f through the injector for Δt, M_{Pi} is the amount of component i going into V_f through the producer for Δt, and M_{ti} is the amount of component i transferred from V_m to V_f through the matrix/fracture interface for Δt.

When this material balance is applied to a time interval Δt, during which flow in V_f is a (pseudo)steady state, ΔM_{fi} values are zero for all i. Then, M_{ti} can be calculated from M_{Ii} and M_{Pi}, which are measurable. How much of the injected amount is actually imbibed into V_m is quantified by the imbibed fraction for component i (F_i). F_i is defined for Δt as

$$F_i = -M_{ti}/M_{Ii}, \quad \ldots\ldots (7)$$

for $i = 1$ and 3. This imbibed fraction is an "apparent" value because M_{ti} is the net amount of mass transfer from V_m to V_f, and because the gross amounts of mass transfer between V_m and V_f for Δt are unknown in general. F_i for surfactant was easy to obtain from the surfactant amount in the produced aqueous phase measured by high-performance liquid chromatography.

Experimental Results and Material-Balance Analysis

This section presents the main results of the flooding/soaking experiments with the 2-EH-4PO-15EO solutions for the two cases: Case 1, the flooding/soaking experiment with initial water in the core, and Case 2, without initial water in the core. The material-balance analysis was used to interpret the results.

Table 3 shows the cumulative improved-oil-recovery factors by surfactant injection and chase RB injection for Case 1, which were calculated by using the original oil amount in the matrix (OOIM). During the surfactant injection before the first soaking period, the injected volume exceeded the volume between the inlet and the outlet line of the core holder by 0.06×10^{-6} m^3. The additional injected volume and the oil recovery associated with it were considered for the subsequent soaking period for oil-recovery calculation and mass-balance calculation. The incremental oil recovery was 33.48% of OOIM after the first soaking period, 29.55% of OOIM after the second soaking period, and 13.08% of OOIM after the third soaking period. The total improved oil recovery was 76.11% of OOIM. It is clear that the surfactant increased oil recovery beyond what the RB injection could recover.

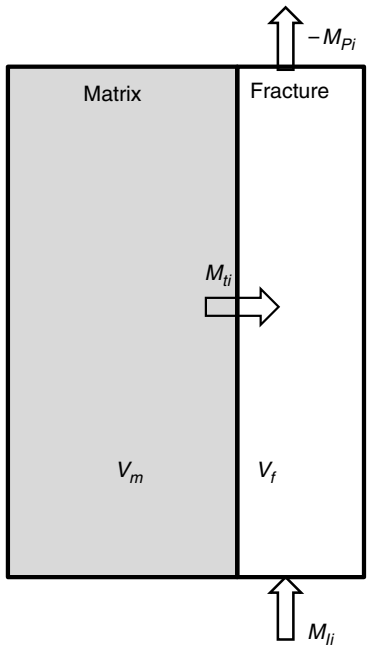

Fig. 5—Schematic of the flooding/soaking experiment. The system consists of two subvolumes: the fracture and matrix volumes. The fracture volume is connected to the injector (source) and the producer (sink).

	Cumulative Improved-Oil-Recovery Factor by Surfactant Solution	F_1	F_1/L (m^{-1})	F_3	F_3/L (m^{-1})	S_w
After the first soaking period	0.3348	0.0178	0.343	0.5000	9.616	0.4658
After the second soaking period	0.6303	0.0175	0.336	0.2131	4.098	0.7031
After the third soaking period	0.7611	0.0061	0.118	–	–	0.8082

Table 3—Experimental results and material-balance analysis for Case 1 (with initial water in the matrix). F_i is defined in Eq. 7.

Table 4 presents the cumulative improved-oil-recovery factors by surfactant injection and chase RB injection for Case 2. During the surfactant injection before the first soaking period, the injected volume exceeded the volume between the inlet and the outlet line of the core holder by 0.75×10^{-6} m^3. Similarly, during the chase RB injection after the second soaking period, the injected volume exceeded by 0.65×10^{-6} m^3. Similar to Case 1, these additional injected volumes and the oil recovery associated with them were considered for the subsequent soaking period for oil-recovery calculation and mass-balance calculation. The incremental oil recovery was 35.55% of OOIM after the first soaking period, 30.51% of OOIM after the second soaking period, and 12.36% of OOIM after the third soaking period. The total improved oil recovery was 78.42% of OOIM. The improved-oil-recovery factors of Cases 1 and 2 were similar to each other, assuming that the effect of the additional injection that occurred for Case 2 was insignificant.

	Cumulative Improved-Oil-Recovery Factor by Surfactant Solution	F_1	F_1/L (m^{-1})	F_3	F_3/L (m^{-1})	S_w
After the first soaking period	0.3555	0.0443	0.382	0.4295	3.703	0.3555
After the second soaking period	0.6606	0.0457	0.394	0.2450	2.112	0.6606
After the third soaking period	0.7842	0.0119	0.103	–	–	0.7842

Table 4—Experimental results and material-balance analysis for Case 2 (without initial water in the matrix). F_i is defined in Eq. 7.

Fig. 6a shows the improved-oil-recovery factors with respect to M_{I3} for both cases. M_{I3} was calculated on a cumulative basis, for which the time interval (Δt) started at the beginning of the surfactant-solution injection. M_{I3} for Case 2 was larger because there was the additional injected volume of surfactant solution (0.75×10^{-6} m^3) before the first soaking period, as previously mentioned. Fig. 6b shows that the use of the surfactant was more efficient for a given amount of oil recovery with no initial water in the matrix. The vertical increase in oil recovery at the same amount of M_{I3} in Fig. 6 corresponds to the improved oil recovery before and after the chase RB injection. It indicates that the imbibition of brine continued during the soaking period after the chase RB injection.

Tables 3 and 4 also provide the F_1 and F_3 values from the material balance for both cases. The calculation of F_i was performed separately for each soaking period. For Case 1, F_3 was 0.5000 after the first soaking period and 0.2131 after the second soaking period. For Case 2, F_3 was 0.4295 after the first soaking period and 0.2450 after the second soaking period. The efficiency of the surfactant imbibition into the matrix decreased after each soaking period for both cases. F_3 values of Case 2 were slightly lower than that of Case 1 after the first soaking period. This indicates that the initial efficiency of the surfactant imbibition increased when brine was initially present in the matrix.

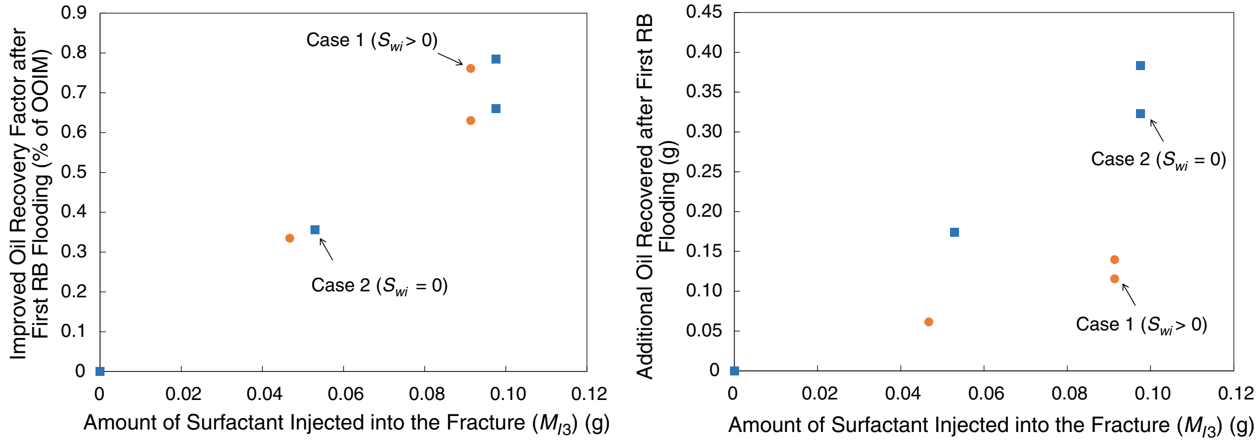

Fig. 6—Oil recovery with respect to the amount of surfactant injected into the fracture for Cases 1 and 2: (a) oil-recovery factor with respect to OOIM and (b) oil recovery (in g).

For Case 1, F_1 was 0.0178 after the first soaking period, 0.0175 after the second soaking period, and 0.0061 after the third soaking period. For Case 2, F_1 was 0.0443 after the first soaking period, 0.0457 after the second soaking period, and 0.0119 after the third soaking period. These results confirmed that the imbibition of brine continued after the surfactant injection was terminated. Also, the F_1 values of Case 1 were systematically lower than those of Case 2. The imbibition of RB was more efficient when there was no initial water in the matrix. A possible reason is that the presence of initial water in the matrix increased the initial efficiency of the surfactant imbibition, resulting in higher surfactant concentration in the matrix. However, the efficiency of RB imbibition was decreased when the IFT between the oleic and aqueous phases was reduced by the larger amount of surfactant imbibed into the matrix. Another possible reason is that capillary force was decreased because of the presence of initial water in the matrix, resulting in weaker RB imbibition. The water-saturation results given in Tables 3 and 4 indicate that the two cases reached similar values of final water saturation; that is, the surfactant injection for a given amount of oil recovery was more efficient when brine was not initially present in the matrix, as shown in Fig. 6b.

Discussion

Among other factors, the results presented in the section Experimental Results and Material-Balance Analysis are affected by the partition coefficient of the surfactant between brine and oil, and the dimensions of the core samples. Their effect on the improved oil recovery and F_i are discussed in this section.

Effect of Partition Coefficient of Surfactant on Improved Oil Recovery and F_i. In the section Experimental Results and Material-Balance Analysis, it was assumed that 2-EH-4PO-15EO was only present in the aqueous phase. The F_i for surfactant was obtained from the surfactant amount in the aqueous phase produced. However, 2-EH-4PO-15EO can partition into both the aqueous and oleic phases, which affects the calculation of improved oil recovery and the F_3 value for the surfactant.

Recently, Baek et al. (2020) measured partition coefficients of 2-EH-7PO-15EO between brine and heavy oil at room temperature. The partition coefficient K is defined as

$$K = C_o / C_w, \quad (8)$$

where C_o and C_w are the concentrations of surfactant in the oleic and aqueous phases, respectively. The partition coefficient was measured to be 1.76 when the initial surfactant concentration in the aqueous phase was 0.5 wt%.

In this subsection, the partition coefficient of 2-EH-4PO-15EO was assumed to be 2.0. Then, the surfactant amount in the oleic phase produced was calculated from the surfactant amount in the aqueous phase produced. The improved oil recovery and F_i values based on this assumed partition coefficient are presented in **Table 5** for Case 1 and **Table 6** for Case 2. Although the improved-oil-recovery factors in Tables 5 and 6 are slightly smaller than those in Tables 3 and 4, the improved-oil-recovery factors of Cases 1 and 2 were still similar to each other. F_1 values in Tables 5 and 6 are the same as those in Tables 3 and 4; hence, F_1 was little affected by the partition coefficient of the surfactant. F_3 values in Tables 5 and 6 are slightly smaller than those in Tables 3 and 4. However, F_3 values for Case 2 were still slightly lower than those of Case 1 after the first soaking period. These results indicate that the improved-oil-recovery factor and F_3 decrease when the partition coefficient was taken into account in the calculation. However, the effect of the surfactant partition coefficient on the calculation of the improved oil recovery and F_i values is small.

	Cumulative Improved-Oil-Recovery Factor by Surfactant Solution	F_1	F_3	S_w
After the first soaking period	0.3314	0.0178	0.4867	0.4630
After the second soaking period	0.6208	0.0175	0.1880	0.6954
After the third soaking period	0.7511	0.0061	–	0.8001

Table 5—Experimental results and material-balance analysis for Case 1 (with initial water in the matrix) when the partition coefficient of 2-EH-4PO-15EO is 2.0.

	Cumulative Improved-Oil-Recovery Factor by Surfactant Solution	F_1	F_3	S_w
After the first soaking period	0.3504	0.0443	0.3824	0.3504
After the second soaking period	0.6491	0.0457	0.1757	0.6491
After the third soaking period	0.7721	0.0119	–	0.7721

Table 6—Experimental results and material-balance analysis for Case 2 (without initial water in the matrix) when the partition coefficient of 2-EH-4PO-15EO is 2.0.

In this research, we did not compare different surfactants with different partition coefficients. The surfactant partition coefficient likely affects the mechanism of oil recovery because it will affect the intraphase and interphase mass-transfer rates and the interaction with rock surfaces through the aqueous and oleic phases. However, it is beyond the scope of the current paper to investigate the effect of surfactant properties on oil recovery in dynamic imbibition experiments.

Effect of Core Length on F_i. In this research, the two cores for Cases 1 and 2 have different lengths: 0.0520 m for Case 1 and 0.1160 m for Case 2. This subsection discusses the effect of the core length on F_i.

F_i for $i = 1$ and 3 can be expressed as

$$F_i = -M_{ti}/M_{Ii} = -A_f \int_0^t \vec{N}_i dt/M_{Ii} = -2Ld \int_0^t \vec{N}_i dt/M_{Ii}, \quad (9)$$

where A_f is the area of the matrix/fracture interface, L is core length, and $\vec{N}_i$ is the mass flux of component i across the matrix/fracture interface. For a given M_{Ii}, F_i increases with increasing core length. Therefore, F_i values are normalized by L for a fair comparison between the cases.

Tables 3 and 4 present F_1/L and F_3/L for both cases. For Case 1, F_3/L was 9.616 m^{-1} after the first soaking period and 4.098 m^{-1} after the second soaking period. For Case 2, F_3/L was 3.703 m^{-1} after the first soaking period and 2.112 m^{-1} after the second soaking period. F_3/L values of Case 2 were systematically lower than those of Case 1, indicating that the efficiency of the surfactant imbibition increased when brine was initially present in the matrix.

For Case 1, F_1/L was 0.343 m^{-1} after the first soaking period, 0.336 m^{-1} after the second soaking period, and 0.118 m^{-1} after the third soaking period. For Case 2, F_1/L was 0.382 m^{-1} after the first soaking period, 0.394 m^{-1} after the second soaking period, and 0.103 m^{-1} after the third soaking period. F_1/L values of Case 1 were lower than those of Case 2 after the first and second soaking periods. They were similar after the third soaking period. The imbibition of RB during the surfactant-injection period was more efficient when there was no initial water in the matrix. The possible reason has been discussed in the section Experimental Results and Material-Balance Analysis.

Conclusions

The main objective of this research was to evaluate how the presence of initial water affects the oil recovery from tight matrices by the imbibition of nonionic-surfactant solution. Two flooding/soaking experiments with 1.0-wt% nonionic-surfactant solution were performed with/without initial water in the matrix. Experimental results were analyzed by the material balance for the components oil, brine, and surfactant. The analysis enabled us to quantitatively evaluate the imbibed fraction of the components injected (brine and chemical). The main conclusions are as follows:

1. The surfactant enhanced the brine imbibition into the matrix through wettability alteration. It increased oil recovery beyond what the RB injection could recover.
2. The initial efficiency of the surfactant imbibition increased when brine was initially present in the matrix. For example, F_3 after the first soaking period was 0.5000 for Case 1 and 0.4295 for Case 2.
3. RB imbibition was more efficient with no initial water in the matrix. A possible reason is that the presence of initial water in the matrix was able to increase the initial efficiency of the surfactant imbibition. However, the increased amount of surfactant in the matrix lowered the IFT between the aqueous and oleic phases and, therefore, the efficiency of RB imbibition was reduced. Another possible reason is that the capillary force was lower in the presence of initial water in the matrix, resulting in weaker imbibition of brine.
4. The two cases (with/without initial water in the matrix) showed different characteristics of the mass transfer through the fracture/matrix interface. The initial surfactant imbibition was more efficient and RB imbibition was less efficient with the presence of initial water in the matrix. However, they resulted in similar values of final water saturation; that is, the surfactant injection was more efficient for a given amount of oil recovery when there was no initial water in the matrix.

Nomenclature

A = area, m^2
b = fracture aperture, m
C = concentration of surfactant, kg/m^3
d = core diameter, m
F = apparent imbibed fraction
k = permeability, darcies
K = partition coefficient of surfactant
L = core length, m
M = mass, kg
N = mass flux, $kg/m^2{\cdot}s$
S = saturation
S_w = water saturation

t = duration, seconds
V = volume, m^3
ρ = density, kg/m^3

Subscripts

e = effective
f = fracture
i = index for pseudocomponent
I = injected
m = matrix
o = oleic phase
P = produced
t = transfer
w = aqueous phase

Acknowledgments

Author Ryosuke Okuno holds the Pioneer Corporation Faculty Fellowship in Petroleum Engineering at the University of Texas at Austin, Austin, Texas, USA.

References

Abedi, B., Castano, E. P. M., Heidaryan, E. et al. 2020. Pore-Scale Visualization on Polymer Flooding: Application of Singular Value Decomposition-Based Image Analysis Method. *J Porous Media* **23** (6): 531–543. https://doi.org/10.1615/JPorMedia.2020033831.

Akin, S., Schembre, J. M., Bhat, S. K. et al. 2000. Spontaneous Imbibition Characteristics of Diatomite. *J Pet Sci Eng* **25** (3–4): 149–165. https://doi.org/10.1016/S0920-4105(00)00010-3.

Alharthy, N., Teklu, T., Kazemi, H. et al. 2015. Enhanced Oil Recovery in Liquid-Rich Shale Reservoirs: Laboratory to Field. Paper presented at the SPE Annual Technical Conference and Exhibition, Houston, Texas, USA, 28–30 September. SPE-175034-MS. https://doi.org/10.2118/175034-MS.

Alvarez, J. O. and Schechter, D. S. 2016. Wettability, Oil and Rock Characterization of the Most Important Unconventional Liquid Reservoirs in the United States and the Impact on Oil Recovery. Paper presented at the SPE/AAPG/SEG Unconventional Resources Technology Conference, San Antonio, Texas, USA, 1–3 August. URTEC-2461651-MS. https://doi.org/10.15530/URTEC-2016-2461651.

Alvarez, J. O. and Schechter, D. S. 2017. Wettability Alteration and Spontaneous Imbibition in Unconventional Liquid Reservoirs by Surfactant Additives. *SPE Res Eval & Eng* **20** (1): 107–117. SPE-177057-PA. https://doi.org/10.2118/177057-PA.

Alvarez, J. O., Neog, A., Jais, A. et al. 2014. Impact of Surfactants for Wettability Alteration in Stimulation Fluids and the Potential for Surfactant EOR in Unconventional Liquid Reservoirs. Paper presented at the SPE Unconventional Resources Conference, The Woodlands, Texas, USA, 1–3 April. SPE-169001-MS. https://doi.org/10.2118/169001-MS.

Alvarez, J. O., Saputra, I. W. R., and Schechter, D. S. 2018a. The Impact of Surfactant Imbibition and Adsorption for Improving Oil Recovery in the Wolfcamp and Eagle Ford Reservoirs. *SPE J.* **23** (6): 2103–2117. SPE-187176-PA. https://doi.org/10.2118/187176-PA.

Alvarez, J. O., Tovar, F. D., and Schechter, D. S. 2018b. Improving Oil Recovery in the Wolfcamp Reservoir by Soaking/Flowback Production Schedule with Surfactant Additives. *SPE Res Eval & Eng* **21** (4): 1083–1096. SPE-187483-PA. https://doi.org/10.2118/187483-PA.

Babadagli, T. 2005. Analysis of Oil Recovery by Spontaneous Imbibition of Surfactant Solution. *Oil & Gas Science and Technology–Rev. IFP* **60** (4): 697–710. https://doi.org/10.2516/ogst:2005049.

Barba, R. E. 2015. Liquids Rich Organic Shale Recovery Factor Application. Paper presented at the SPE Annual Technical Conference and Exhibition, Houston, Texas, USA, 28–30 September. SPE-174994-MS. https://doi.org/10.2118/174994-MS.

Baek, K., Argüelles-Vivas, F. J., Abeykoon, G. A. et al. 2020. Low-Tension Polymer Flooding Using Short-Hydrophobe Surfactant for Heavy Oil Recovery. *Energy & Fuels* (in press; published 23 November 2020). https://doi.org/10.1021/acs.energyfuels.0c02720.

Bowker, K. A. 2003. Recent Development of the Barnett Shale Play, Fort Worth Basin. *West Texas Geological Society Bull.* **42** (6): 4–11.

Cheng, Y., Zhang, C., and Zhu, L. 2017. A Fractal Irreducible Water Saturation Model for Capillary Tubes and Its Application in Tight Gas Reservoir. *J Pet Sci Eng* **159** (November): 731–739. https://doi.org/10.1016/j.petrol.2017.09.079.

Cil, M., Reis, J. C., Miller, M. A. et al. 1998. An Examination of Countercurrent Capillary Imbibiton Recovery from Single Matrix Blocks and Recovery Predictions by Analytical Matrix/Fracture Transfer Functions. Paper presented at the SPE Annual Technical Conference and Exhibition, New Orleans, Louisiana, USA, 27–30 September. SPE-49005-MS. https://doi.org/10.2118/49005-MS.

Gao, Z. and Hu, Q. 2016. Initial Water Saturation and Imbibition Fluid Affect Spontaneous Imbibition into Barnett Shale Samples. *J Nat Gas Sci Eng* **34** (August): 541–551. https://doi.org/10.1016/j.jngse.2016.07.038.

Ghanbari, E. and Dehghanpour, H. 2015. Impact of Rock Fabric on Water Imbibition and Salt Diffusion in Gas Shales. *Int J Coal Geol* **138** (15 January): 55–67. https://doi.org/10.1016/j.coal.2014.11.003.

Kathel, P. and Mohanty, K. K. 2013. Wettability Alteration in a Tight Oil Reservoir. *Energy Fuels* **27** (11): 6460–6468. https://doi.org/10.1021/ef4012752.

Li, K. and Li, Y. 2014. Effect of Initial Water Saturation on Crude Oil Recovery and Water Cut in Water-Wet Reservoirs. *Int J Energy Res* **38** (12): 1599–1607. https://doi.org/10.1002/er.3182.

Liu, J., Sheng, J. J., Wang, X. et al. 2019. Experimental Study of Wettability Alteration and Spontaneous Imbibition in Chinese Shale Oil Reservoirs Using Anionic and Nonionic Surfactants. *J Pet Sci Eng* **175** (April): 624–633. https://doi.org/10.1016/j.petrol.2019.01.003.

Mejia, M. 2018. *Experimental Investigation of Surfactant Flooding in Fractured Limestones*. Master's thesis, University of Texas at Austin, Austin, Texas, USA (December 2018).

Morsy, S., Sheng, J. J., and Soliman, M. Y. 2013. Waterflooding in the Eagle Ford Shale Formation: Experimental and Simulation Study. Paper presented at the SPE Unconventional Resources Conference and Exhibition-Asia Pacific, Brisbane, Australia, 11–13 November. SPE-167056-MS. https://doi.org/10.2118/167056-MS.

Pettit, J., Tavallali, M., and Muirhead, M. 2016. Permian Basin Technical Issues: (Part 1) How To Manage Water Cut. IHS Markit, 27 December 2016, https://ihsmarkit.com/research-analysis/permian-basin-technical-issues-part-1-how-to-manage-water-cut.html (accessed 14 November 2019).

Rassenfoss, S. 2018. Rising Tide of Produced Water Could Pinch Permian Growth. *J Pet Technol* 12 June 2018, https://pubs.spe.org/en/jpt/jpt-article-detail/?art=4273 (accessed 14 November 2019).

Standnes, D. C. and Austad, T. 2000. Wettability Alteration in Chalk: 2. Mechanism for Wettability Alteration from Oil-Wet to Water-Wet Using Surfactants. *J Pet Sci Eng* **28** (3): 123–143. https://doi.org/10.1016/S0920-4105(00)00084-X.

Tong, Z., Xie, X., and Morrow, N. R. 2001. Scaling of Viscosity Ratio for Oil Recovery by Imbibition from Mixed-Wet Rocks. Paper presented at the International Symposium of the Society of Core Analysis, Edinburgh, UK, 17–19 September. SCA 2001–21.

Viksund, B. G., Morrow, N. R., Ma, S. et al. 1998. Initial Water Saturation and Oil Recovery from Chalk and Sandstone by Spontaneous Imbibition. Paper presented at the International Symposium of the Society of Core Analysts, The Hague, The Netherlands, 14–16 September. SCA-9814.

Wang, M., Abeykoon, G. A., Argüelles-Vivas, F. J. et al. 2019a. Ketone Solvent as a Wettability Modifier for Improved Oil Recovery from Oil-Wet Porous Media. *Fuel* **258** (15 December): 116195. https://doi.org/10.1016/j.fuel.2019.116195.

Wang, M., Baek, K., Abeykoon, G. A. et al. 2019b. Comparative Study of Ketone and Surfactant for Enhancement of Water Imbibition in Fractured Porous Media. *Energy Fuels* **34** (5): 5159–5167. https://doi.org/10.1021/acs.energyfuels.9b03571.

Yarveicy, H. and Haghtalab, A. 2018. Effect of Amphoteric Surfactant on Phase Behavior of Hydrocarbon-Electrolyte-Water System—An Application in Enhanced Oil Recovery. *J Dispers Sci Technol* **39** (4): 522–530. https://doi.org/10.1080/01932691.2017.1332525.

Yarveicy, H. and Javaheri, A. 2019. Application of Lauryl Betaine in Enhanced Oil Recovery: A Comparative Study in Micromodel. *Petroleum* **5** (2): 123–127. https://doi.org/10.1016/j.petlm.2017.09.004.

Yarveicy, H., Habibi, A., Pegov, S. et al. 2018. Enhancing Oil Recovery by Adding Surfactants in Fracturing Water: A Montney Case Study. Paper presented at the SPE Canada Unconventional Resources Conference, Calgary, Alberta, Canada, 13–14 March. SPE-189829-MS. https://doi.org/10.2118/189829-MS.

Zeng, T., Miller, C. S., and Mohanty, K. K. 2018. Application of Surfactants in Shale Chemical EOR at High Temperatures. Paper presented at the SPE Improved Oil Recovery Conference, Tulsa, Oklahoma, USA, 14–18 April. SPE-190318-MS. https://doi.org/10.2118/190318-MS.

Zhou, X., Morrow, N. R., and Ma, S. 2000. Interrelationship of Wettability, Initial Water Saturation, Aging Time, and Oil Recovery by Spontaneous Imbibition and Waterflooding. *SPE J*. **5** (2): 199–207. SPE-62507-PA. https://doi.org/10.2118/62507-PA.